

## Characterization, Electrical and Magnetic Properties of Nd<sub>2</sub>Zr<sub>2</sub>O<sub>7</sub> Compound

POOJA RAGHUVANSHI, A.N. THAKUR\* and PRIYANKA RANI

Department of Physics, Tilak Dhari Post Graduate College, Jaunpur-222 002, India

\*Corresponding author: E-mail: ant\_tdc@yahoo.com

(Received: 14 April 2012;

Accepted: 6 February 2013)

AJC-12935

The Nd<sub>2</sub>Zr<sub>2</sub>O<sub>7</sub> compound is prepared by using solid state reaction technique. Its structural and electrical properties have been investigated. X-ray diffraction pattern indicates that Nd<sub>2</sub>Zr<sub>2</sub>O<sub>7</sub> crystallizes in an orthorhombic perovskite structure. The compound was characterized through powder differential thermal analysis, thermogravimetric analysis and derivative thermogravimetry. The electrical conductivity ( $\sigma$ ), dielectric constant ( $\epsilon'$ ), dielectric loss ( $\epsilon''$ ) and quality factor (Q) of Nd<sub>2</sub>Zr<sub>2</sub>O<sub>7</sub> was measured in the temperature range 300-1125K at an internal frequency of 1 kHz. The  $\log \sigma$  vs.  $10^3/T$  plot yield two different slopes separated by break temperature ( $T_1$ ). The activation energy below and above  $T_1$  have been estimated as 0.13 eV and 2.1 eV respectively. Hence the electrical conductivity below  $T_1$  is essentially extrinsic always associated with impurities, defects and interstitials and conductivity above  $T_1$  is essentially intrinsic due to the change in conduction mechanism. The magnetic susceptibility of the compound was measured in the temperature range 300-1100 K at field 1.55  $\times 10^{-1}$  Tesla. The magnetism in this compound arises from the rare-earth ions, while Zr is non magnetic.

**Key Words:** X-ray diffraction, Differential thermal analysis, Thermogravimetric analysis, Derivative thermogravimetry, Nd<sub>2</sub>Zr<sub>2</sub>O<sub>7</sub>.

### INTRODUCTION

Pyrochlores with the general formula A<sub>2</sub>B<sub>2</sub>O<sub>7</sub> have many potential technological applications because of their refractory nature and their interesting electronic properties, which vary from insulating through semiconductor to metal-like depending on the chemical composition<sup>1</sup>. Lanthanide pyrochlores, in which the light lanthanide elements (La to Gd) can occupy the A position, are well known for their magnetic behaviour at low temperature and their fluorescent phosphorescent behaviour<sup>1</sup>.

These rare earth zirconium oxides have complex chemistry, low thermal conductivity, high melting point, high thermal expansion coefficient, high stability and ability to accommodate defects<sup>2</sup>. In view of these important properties, these type of oxides find applications in gas turbines and diesel engines as thermal barrier coating, possible host for radioactive wastes and surplus actinides<sup>2,3</sup>, as hosts for fluorescence centers<sup>4,5</sup>, as oxidation catalysts<sup>6</sup>, as oxygen monitoring sensors and as solid electrolytes in high temperature fuel cells<sup>7</sup>. In this paper, we discussed the synthesis, characterization, electrical and magnetic properties of Nd<sub>2</sub>Zr<sub>2</sub>O<sub>7</sub> compound.

### EXPERIMENTAL

**Sample preparation and characterization:** Powdered sample of Nd<sub>2</sub>Zr<sub>2</sub>O<sub>7</sub> was synthesized by means of a solid state

using Nd<sub>2</sub>O<sub>3</sub> (99.99 % Alfa Aesar ) and ZrO<sub>2</sub> (99.7 % Alfa Aesar ). The stiochiometric amounts of Nd<sub>2</sub>O<sub>3</sub> and ZrO<sub>2</sub> were thoroughly mixed in an agate mortar for 3 h in wet medium and then dried and calcined in alumina crucible at 1300 K for 50 h in air atmosphere followed by one intermediate grinding. The final product was cool down slowly.

The powdered sample was characterized by means of an X-ray diffractometer (thermoelectron-XRL EXTRA) at room temperature using CuK $\alpha$  radiation with  $\lambda = 0.15418$  nm in wide range of Bragg angle ( $10^\circ \leq \theta \leq 90^\circ$ ).

The thermal behaviour of Nd<sub>2</sub>Zr<sub>2</sub>O<sub>7</sub> was studied from 323 to 1123 K using differential thermal analysis, thermogravimetric analysis and differential thermal analysis (Perkin Elemer Pyris). The experiments were conducted in nitrogen gas at a heating rate of 283 K/min and flow rate of 100 mL/min.

**Electrical conductivity measurement:** The electrical conductivity of sample was measured by finding out the resistance of the sample on pressed pellet by two electrode method. The pellet (area -  $0.95 \times 10^{-4}$  m<sup>2</sup> and thickness -  $0.30 \times 10^{-2}$  m) was prepared from homogenous powder of Nd<sub>2</sub>Zr<sub>2</sub>O<sub>7</sub> at isostatic pressure  $7.19 \times 10^8$  Nm<sup>-2</sup> using hydraulic press. The pellet was then sintered at 1500 K in air atmosphere for 30 h. Both the faces of the sintered sample were coated with high purity air drying silver paint after making both surfaces flat and parallel and then inserted between two silver electrodes. The silver foils were electrically insulated from the sample

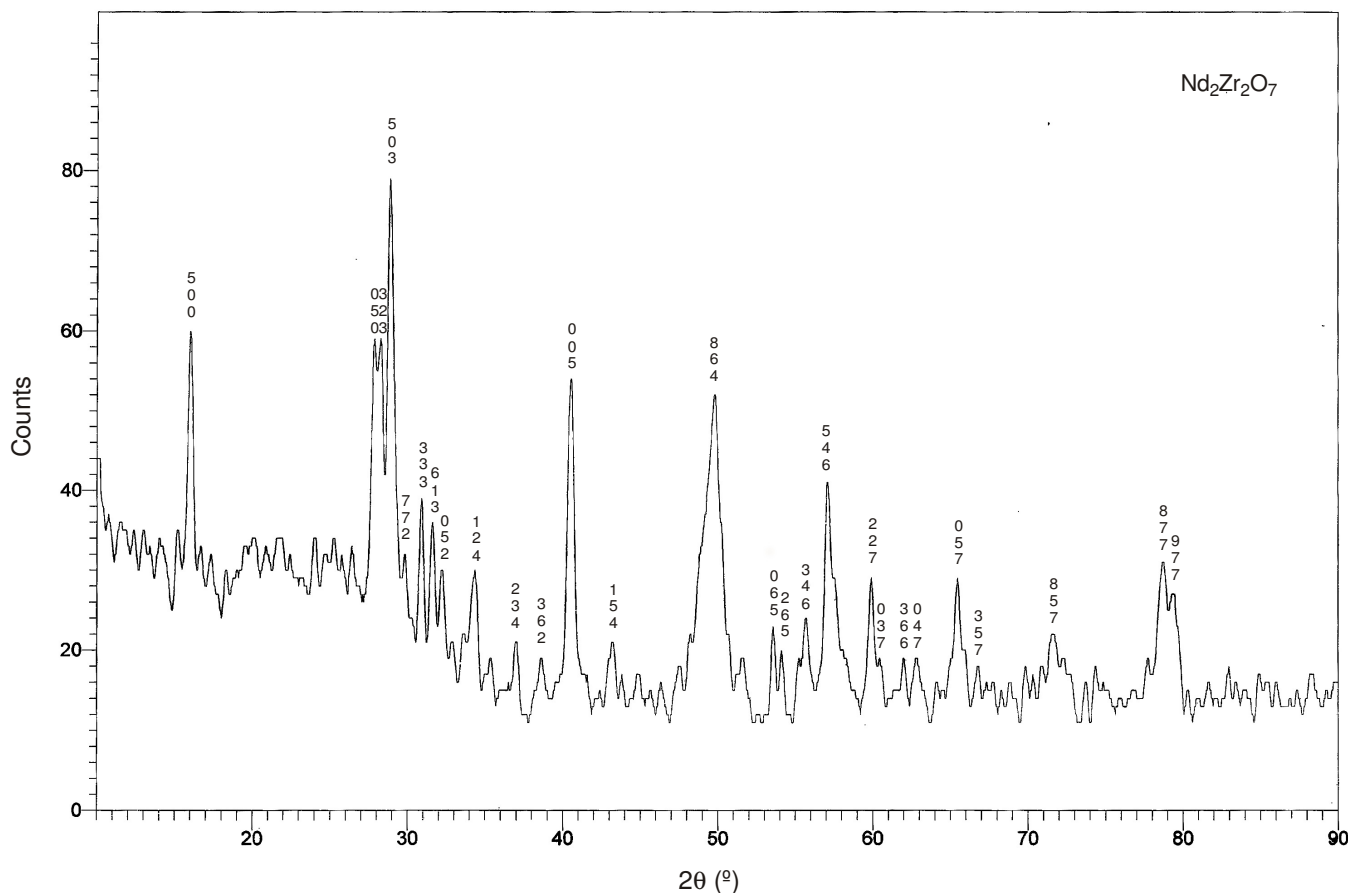


Fig. 1. Room temperature XRD of  $\text{Nd}_2\text{Zr}_2\text{O}_7$

holders by mica sheets. The electrical conductivity was measured by an autocompute LCR-Q meter (Model 928, Systronics India).

**Dielectric measurement:** An autocompute LCR-Q meter (model 928, Systronics India) was used to measure the capacitance ( $c$ ) and quality factor ( $Q$ ) of the sample at different temperature and at a frequency of 1 kHz. The dielectric constant ( $\epsilon'$ ) and dielectric loss ( $\epsilon''$ ) of the sample was calculated by using the following relation<sup>8,9</sup>.

$$\epsilon' = \frac{ct}{\epsilon_0 A} \quad (1)$$

$$\epsilon'' = \frac{\epsilon'}{Q} \quad (2)$$

where  $c$  = the capacitance of the capacitor in Farad,  $t$  = the thickness,  $A$  = face area of the pellet,  $\epsilon_0$  = permittivity of free space and  $Q$  = quality factor respectively.

**Magnetic measurement:** Magnetic susceptibility measurements were done on powdered sample using Faraday's method<sup>10,11</sup>.  $\text{Gd}_2(\text{WO}_4)_3$  has been used for standardization.

## RESULTS AND DISCUSSION

Fig. 1 shows the XRD pattern of  $\text{Nd}_2\text{Zr}_2\text{O}_7$ . From XRD pattern,  $d_{hkl}$  values have been obtained using the relation<sup>12</sup>.

$$d_{hkl} = \frac{0.15418}{2 \sin \theta} \quad (3)$$

From these values of  $d_{hkl}$ , structure of the studied compounds was resolved using usual procedure. All the peaks have

been assigned with proper  $hkl$  values. This confirms that prepared compounds have single phase and no unreacted part of the material was left. The unit cell is orthorhombic and the lattice constant was estimated to be  $a_0 = 2.7695$ ,  $b_0 = 1.6015$  nm and  $c_0 = 1.1135$  nm.

Fig. 2 presents the DTA, TGA and DTG trace of  $\text{Nd}_2\text{Zr}_2\text{O}_7$ . DTA trace show exothermic peak at 348 K and endothermic peaks at 373 K, 628 K and 788 K. The corresponding TGA trace shows weight loss in two successive steps. The first step of weight loss 1.75 % is from 547 K to 663 K due to removal of absorbed water and gaseous species. The second step of weight loss 0.70 % is from 748 K to 833 K and above 833 K the compound is stable. The DTG trace show maximum rate of mass change at 348 K, 373 K, 603 K and 793 K.

Fig. 3 shows the variation of dielectric constant ( $\epsilon'$ ), dielectric loss ( $\epsilon''$ ) and quality factor with temperature at 1 kHz. The dielectric constant of  $\text{Nd}_2\text{Zr}_2\text{O}_7$  at 400 K is 211. At lower temperature the dielectric constant ( $\epsilon'$ ) seems to have almost no temperature dependence, so these values may be taken as the room temperature values of the materials. The reported values of  $\epsilon'$  has been calculated using the capacitance value for the pellet. The density of this pellet remains less than the theoretical density of this material. This means pellets contain air pores. Therefore a correction for pore fraction ( $f_p$ ) is essential to obtain the bulk value of the dielectric constant ( $\epsilon'_b$ ) and is given by relation<sup>13</sup>.

$$f_p = \frac{d_0 - d_p}{d_0} \quad (4)$$

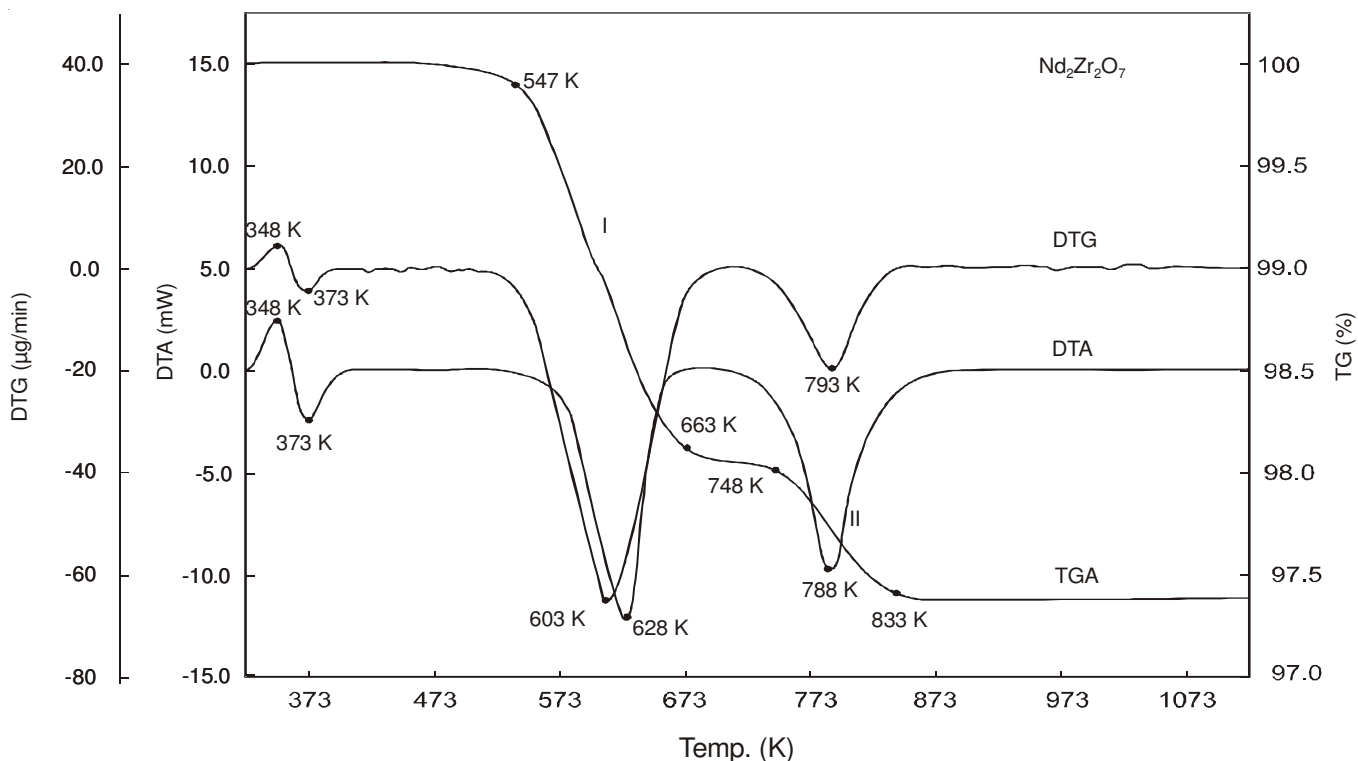


Fig. 2. TGA, DTA and DTG curve of Nd<sub>2</sub>Zr<sub>2</sub>O<sub>7</sub>

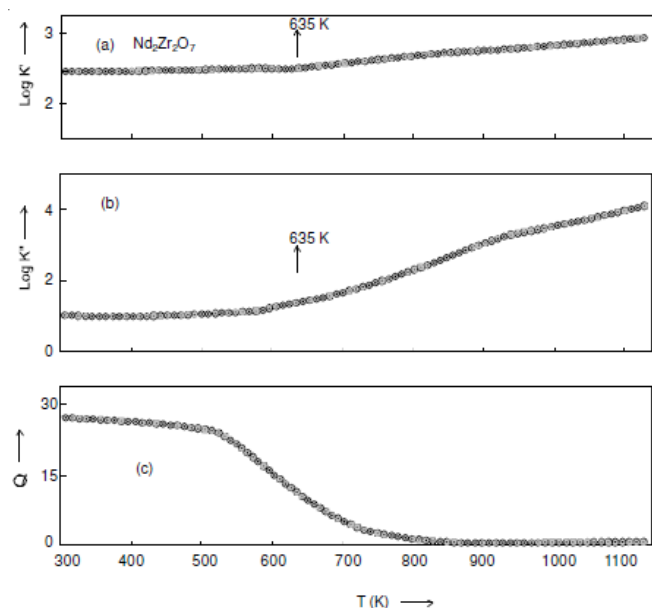


Fig. 3. (a) plots of logarithm of dielectric constant (log k') against absolute temperature (t); (b) plots of logarithm of dielectric loss (log k'') against absolute temperature (t); (c) plots of quality factor (Q) against absolute temperature (t)

The theoretical density ( $d_0$ ), pellet density ( $d_p$ ) and pore fraction of Nd<sub>2</sub>Zr<sub>2</sub>O<sub>7</sub> are  $3.81 \times 10^3 \text{ Kg m}^{-3}$ ,  $3.75 \times 10^3 \text{ Kg m}^{-3}$  and  $f_p = 0.016$  respectively. For low conducting solid  $\epsilon'_b$ ,  $\epsilon'$  and  $f_p$  are related by the relation<sup>14</sup>,

$$\epsilon'_b = \frac{(\epsilon'^{1/3} - f_p)^3}{1 - f_p} \quad (5)$$

The evaluated values of  $\epsilon'_b$  is 284.33.

The values of  $\epsilon'$  become large as temperature is increased and validity of eqn. (5) becomes doubtful. Further this formula

affects only the magnitude but not the nature of temperature variation of  $\epsilon'$ . Therefore we have not used this correction at higher temperatures. The values of dielectric constant ( $\epsilon'$ ) and dielectric loss ( $\epsilon''$ ) at 400 K, 600 K, 800 K and 1000 K at frequency 1 kHz are given in Tables 1 and 2 respectively.

TABLE-1 DIELECTRIC CONSTANT ( $\epsilon'$ ) of Nd <sub>2</sub> Zr <sub>2</sub> O <sub>7</sub> AT DIFFERENT TEMPERATURE				
Compound	400 K	600 K	800 K	1000 K
Nd <sub>2</sub> Zr <sub>2</sub> O <sub>7</sub>	281.84	316.23	398.11	707.95

TABLE-2 DIELECTRIC LOSS ( $\epsilon''$ ) OF Nd <sub>2</sub> Zr <sub>2</sub> O <sub>7</sub> AT DIFFERENT TEMPERATURE				
Compound	400 K	600 K	800 K	1000 K
Nd <sub>2</sub> Zr <sub>2</sub> O <sub>7</sub>	10	17.78	281.84	3162.28

The dielectric constant has very slow increase at lower temperature. This shows that there is no chance for the existence of thermally generated charge carrier at lower side of temperature. Well made electrode rules out the possibility of interfacial polarization. Therefore this slow increase seems to be the combined effect of lattice and electronic polarizability of individual ions. The increase of these polarizabilities seems to compensate the slight decrease of polarizability due to decrease in the number of ions per unit volume following the lattice expansion with temperature. However it must be noticed that the increase of  $\epsilon'$  with T is very slow in comparison to the variation one expects for ionic solids. This indicates that either thermal expansion of these materials is very small or they have some other kind of polarization mechanism.

The dielectric constant ( $\epsilon'$ ) has much faster increase above certain critical temperature ( $T_k = 635$  K). The dielectric loss ( $\epsilon''$ ) shows similar behaviour above  $T_k$ . The rapid increase in dielectric constant above  $T_k$  is due to space charge polarization<sup>15,16</sup>. The pressed sample develops a considerable amount of space charge polarization arising out from the defects or impurities present in the bulk or at the surface of the material.

The electrical conductivity ( $\sigma$ ) have been measured in the temperature range 300-1125 K at frequency 1 kHz. The variation of  $\log \sigma$  vs  $10^3/T$  is shown in Fig. 4. The curve follows the well known exponential relation for semiconductor  $\sigma = \sigma_0 \exp(-E_a/kT)$  but with two different slopes. A kink occurs at  $T_1$  ( $T_1 = 641$  K) termed as break temperature. The pre-exponential constant ( $\sigma_0$ ) and activation energy ( $E_a$ ) have been calculated from the slopes.

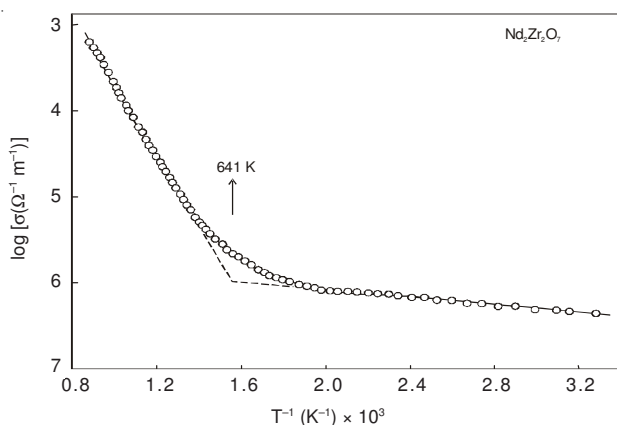


Fig. 4. Plots of logarithm of electrical conductivity ( $\log \sigma$ ) against inverse of absolute temperature ( $T^{-1}$ )

The values of pre exponential constant, activation energy and break temperature have been presented in Table-3.

TABLE-3 ELECTRICAL TRANSPORT PARAMETER OF $\text{Nd}_2\text{Zr}_2\text{O}_7$ COMPOUND					
Compound	Break temperature ( $T_1$ )	For $T < T_1$		For $T > T_1$	
		$\sigma_0$ ( $\Omega^{-1}\text{m}^{-1}$ )	$E_a$ (eV)	$\sigma_0$ ( $\Omega^{-1}\text{m}^{-1}$ )	$E_a$ (eV)
$\text{Nd}_2\text{Zr}_2\text{O}_7$	641	$349.92 \times 10^{-7}$	0.13	$2.88 \times 10^7$	2.1

The electrical conductivity of  $\text{Nd}_2\text{Zr}_2\text{O}_7$  at room temperature is  $\sigma = 10^{-4} \Omega^{-1}\text{m}^{-1}$  which indicate that the compound is insulator. However with increasing temperature their conductivity rapidly increases and becomes conductor.

The activation energy below and above break temperature are nearly 0.13 eV and 2.1 eV respectively. In semiconducting materials, the electrical conduction at low temperature is always associated with impurities, defects and interstitials which generally provide states in forbidden energy gap of the material and lower value of activation energy. The contribution of defects or impurities towards conduction in solid can be explained in terms of donors or acceptors and is represented by expression<sup>17</sup>.

$$\sigma_d = A \exp\left(\frac{-E_i}{KT}\right) \quad (6)$$

where  $E_i$  is ionization energy of donors or acceptors and usually  $E_i$  ca. 0.13 eV for semiconducting material. The activation energy below break temperature is found approximately comparable to the ionization energy  $E_i$  and therefore the conclusion is that electrical conduction is certainly due to impurities, point defects, or interstitials seems to be reasonable.

The activation energy ca. 2.1 eV estimated in the higher temperature range  $T > T_1$  seems to be an intrinsic because  $\sigma_0$  is in the correct range for intrinsic conductivity. Thus the change in the nature of the  $\log \sigma$  vs  $10^3/T$  curve at  $T_1$  is due to the change in the conduction mechanism *i.e.* transition from extrinsic to intrinsic conduction.

The magnetic susceptibility measurement of  $\text{Nd}_2\text{Zr}_2\text{O}_7$  was done in heating and cooling cycles. No hysteresis was observed and  $\chi_M$  values were found to be same in heating and cooling cycles, although a small loss of weight is detected in heating cycle may be due to presence of moisture. The results are shown in Fig. 5 as  $\chi_M^{-1}$  vs  $T$  plots. At higher temperature the  $\chi_M^{-1}$  vs  $T$  plots are linear and obey Curie-Weiss law<sup>16</sup>.

$$\chi_M^{-1} = \frac{T - \theta_p}{C_M} \quad (7)$$

where  $\theta_p$  is paramagnetic Curie temperature and  $C_M$  is the molar Curie constant.

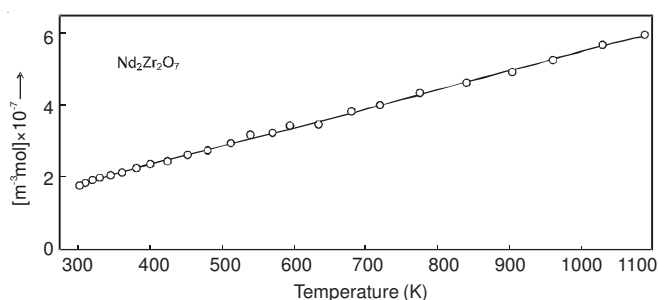


Fig. 5. Variation of inverse of molar magnetic susceptibility ( $\chi_M^{-1}$ ) with absolute temperature of  $\text{Nd}_2\text{Zr}_2\text{O}_7$

$\text{Nd}_2\text{Zr}_2\text{O}_7$  is magnetically simple because magnetism arises from the trivalent rare earth ions *i.e.* the magnetic interaction exists in  $\text{Nd}_2\text{Zr}_2\text{O}_7$  is  $\text{R}^{3+} - \text{R}^{3+}$  (rare-earth ions). Thus at temperature much higher than ordering temperature the molar magnetic susceptibility of  $\text{Nd}_2\text{Zr}_2\text{O}_7$  can be approximated by the relation<sup>18</sup>.

$$\chi_M = \frac{N\mu_0\mu_B^2}{3k} \left[ \frac{\bar{P}^2}{T - \theta_p} \right] \quad (8)$$

where  $N$  is Avagadro number,  $\mu_B$  is Bohr magneton,  $\mu_0$  is permeability constant,  $k$  is Boltzmann constant,  $\bar{P}$  magneton numbers of magnetic ions  $\text{R}^{3+}$  and  $\theta_p$  is the paramagnetic Curie temperature. The eqn. (8) can also be written as:

$$\chi_M^{-1} = \frac{3k(T - \theta_p)}{N\mu_0\mu_B^2\bar{P}^2} \quad (9)$$

Comparing eqn. (7) and (9) we have

$$\bar{C}_M = \frac{N\mu_0\mu_B^2\bar{P}^2}{3k}$$

$$\text{or } \bar{P} = \left[ \frac{3k\bar{C}_M}{N\mu_0\mu_B^2} \right]^{1/2} \quad (10)$$

The experimental value of  $\bar{P}$  can be evaluated from the value of  $\bar{C}_M$  obtained from  $\chi^{-1}_M$  vs T plot. The theoretical value of  $\bar{P}$  has been already known. The theoretical and experimental values of  $\bar{P}$  with magnetic ions are given in Table-4 and the values of  $\theta_p$  and  $\bar{C}_M$  are given in Table-5.

TABLE-4  
MAGNETIC ION WITH THEORETICAL AND EXPERIMENTAL  
VALUE OF AVERAGE MAGNETON NUMBER  $\bar{P}$  OF Nd<sub>2</sub>Zr<sub>2</sub>O<sub>7</sub>

Compounds	Magnetic ion	Theoretical value	Experimental value
Nd <sub>2</sub> Zr <sub>2</sub> O <sub>7</sub>	Nd <sup>3+</sup>	3.62	3.53

TABLE-5  
PARAMAGNETIC CURIE TEMPERATURE ( $\theta_p$ ) AND  
MOLAR CURIE CONSTANT ( $\bar{C}_M$ ) OF Nd<sub>2</sub>Zr<sub>2</sub>O<sub>7</sub>

Compounds	$\theta_p$ (K)	$\bar{C}_M \times 10^5$ (m <sup>3</sup> K mol <sup>-1</sup> )
Nd <sub>2</sub> Zr <sub>2</sub> O <sub>7</sub>	-60	1.95

It is seen from the Table-4 that there is a good agreement between theoretical and experimental values of  $\bar{P}$ , which shows that ionic moment involved in the magnetization process concern the tripositive rare earth ions.

The value of  $\theta_p$  is negative for studied compounds suggesting a possible antiferromagnetic ordering of this compound at lower temperature. However, such small values of  $\theta_p$  can also be due purely to the crystal field effect with a little contribution from simple dipole-dipole interaction between the magnetic ions.

### Conclusion

The powder XRD pattern shows the pyrochlore phase of Nd<sub>2</sub>Zr<sub>2</sub>O<sub>7</sub>. DTA, TGA and DTG studies show that the compound is stable above certain temperature. The dielectric constant ( $\epsilon'$ ) and dielectric loss ( $\epsilon''$ ) have very slow increase upto  $T_k$ . Above  $T_k$  this increase becomes much faster. The reason for faster increase of  $\epsilon'$  and  $\epsilon''$  above  $T_k$  is due to space charge

polarization. The electrical conductivity of Nd<sub>2</sub>Zr<sub>2</sub>O<sub>7</sub> at room temperature is  $10^{-4} \Omega^{-1} \text{m}^{-1}$  which indicate that compound is insulator. However with increasing temperature their conductivity rapidly increases and becomes conductor. Our results reveal that Nd<sub>2</sub>Zr<sub>2</sub>O<sub>7</sub> is a new pyrochlore antiferromagnet.

### ACKNOWLEDGEMENTS

The authors are grateful to Prof. K. Das and Mr. N.K. Das, Central Research facility, IIT Kharagpur for providing DTA, TGA and DTG facility and Mr. U.S.Singh, IIT Kanpur for providing XRD facility.

### REFERENCES

1. M.A. Subramanian, G. Aravamundan and G.V. Subbarao, *Prog. Solid State Chem.*, **15**, 55 (1983).
2. R. Vassen, X. Cao, F. Tietz, D. Basu and D. Stover, *J. Am. Ceram. Soc.*, **83**, 2023 (2000).
3. K.E. Sickafus, L. Miniervini, R.W. Grimes, J.A. Valdez, M. Ishimaru, F. Li, K.J. McClellan and T. Hartmann, *Science*, **289**, 748 (2000).
4. O. Otaki, T. Hoshikawa, M. Shimada and K. Koizumi, *J. Ceram. Soc. Jpn.*, **96**, 124 (1996).
5. R.A. McCauley and F.A. Hummel, *J. Lumin.*, **6**, 105 (1972).
6. S.J. Korf, H.J.A. Koopmans, B.C. Lippens, A.J. Burggras and P.J. Gellings, *J. Chem. Soc., Faraday Trans. 1*, **83**, 1485 (1987).
7. K.J. de Vries, T. Van Dijk, A.J. Burggraaf, *Fast Ion Transport in Solids*, Elsevier, North Holland (1979).
8. M. Cusack, *The Electrical and Magnetic Properties of Solids* (London: Longmans) (1967).
9. J.P. Suchet, *Electrical Conduction in Solids Materials*, London Pergamon (1975).
10. L.F. Bates, *Modern Magnetism* London, Cambridge (1951).
11. A.N. Thakur, K. Gaur, M.A. Khan and H.B. Lal, *Indian J. Phys.*, **71A**, 91 (1997).
12. C. Kittel, *Introduction to Solid State Physics*, John Wiley & Sons, Inc., edn. 7 (1996).
13. A.N. Thakur, K. Gaur and H.B. Lal, *Indian J. Phys.*, **70A**, 225 (1996).
14. V.P. Srivastava, PhD. Thesis, University of Gorakhpur, India (1998).
15. N.M.L. Goswami, R.N.P. Choudhary and P.K. Mahapatra, *Indian J. Phys.*, **73A**, 445 (1999).
16. N.K. Singh, S. Sharma and R.N.P. Choudhary, *Indian J. Phys.*, **74**, 63 (2000).
17. A.J. Dekker, *Solid State Physics*, MacMillan, London (1964).
18. A.N. Thakur, K. Gaur, M.A. Khan and H.B. Lal, *Indian J. Phys.*, **71A**, 91 (1997).